



Numerical Simulation and Design for Highly Precise Control of Temperature for an Air-conditioning System in a Laboratory Environment

Zong-Da Tsai^{a,b}, Ching-Yuarn Liu, Yen-Ching Chung, Ching-Wei Hsu and Yung-Chiang Chang

^aNational Synchrotron Radiation Research Center (NSRRC), Hsinchu 30076, Taiwan, R.O.C.

^bE-Mail: ZDTsai@nsrrc.org.tw

The civil construction and utility systems of the 3-GeV Taiwan Photon Source (TPS) at NSRRC are ready for machine commission in 2014. Because various accelerator facilities are sensitive to temperature, its control and the associated design must be considered carefully. For this object, much effort is devoted to promote the temperature stability of the air-conditioning system. A highly precise temperature control ± 0.01 °C has been achieved to meet a more critical stability requirement. Analysis of the characteristics between the control valves and the heat exchanger and application of a specified control philosophy can effectively minimize the temperature variation. Here we discuss the mechanism through numerical simulation of thermal sources and flow, and verify the practical influences to achieve a significantly improved stability of temperature in a laboratory environment.

Temperature stability related to time

We analyzed the relation between valves and heat exchangers, including the range ability, dead band, hysteresis and authority characteristics. The two control valves with an equal percentage type have been selected corresponding to cooling or heating exchangers. The larger valve is responsible for a large temperature fluctuation such as on-off thermal loading. The smaller valve is responsible for fine tuning with an oscillating valve control. The scheme of the AHU and control system is shown in Figure 1.

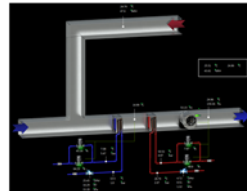


Figure 1: Scheme of the AHU and control system

The air flow via the cooling coil is based on the dew-point temperature for humidity control. According to the temperature feedback in the inlet air duct, the supply air via the heating coil must be well controlled better than ± 0.1 °C. The sensor locations must be chosen carefully to enable a sufficiently rapid response to regulate the control valve; a slow response would create difficulty for fine tuning. For each coil with two control valves having seamless integration without jumps and drifts, we implemented a fuzzy algorithm into the controller to obtain great integration between two valves. The smaller valve is applied a traditional PID algorithm to fine-tune the temperature variation below ± 0.1 °C, as shown in Figure 2. The outlet air temperature also attains variations ± 0.01 °C. Figure 3 shows that the fluctuation caused by a door opening can be damped within 15 min; a stable temperature is then maintained.

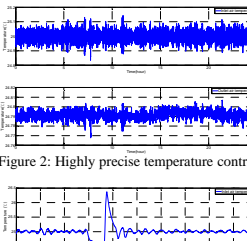


Figure 2: Highly precise temperature control

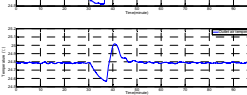


Figure 3: Transient variation of temperature with a fluctuation caused by a door opening

Model Construction and Boundary Conduction

The outlet air duct is located at the top-right side with a concave area. A fabric porous air duct is adopted for the inlet air duct (diameter 760 mm). The 13 rectangular outlet air openings are distributed at bottom-left sides (each of width 600 mm, length 900 mm). The laboratory space has total volume 230 m³ and the air change can attain 58 cycles per hour. To understand the uniformity of the air flow and temperature distribution, we created two models to implement numerical simulation. In case 1, the model analyzes the trend of cooling over a duration 300 s and observes the transient distribution of the air temperature and velocity when the room is cooled from 30 to 20 °C. In case 2, the model incorporates a 1000-W source of heat and maintains the temperature of the room at 25 °C. We observe a steady distribution of air temperature and velocity. The boundary conditions are shown in Tables 1 and 2. We neglect the effect of thermal conduction of each wall but take account of the effects of the buoyancy and gravity of hot air.

Simulation Results and Discussion

In case 1, because of the variation of density between hot and cold air, the air flows toward the bottom and then goes to air openings at the left side in the preceding 30 s. During this interval, the air velocity is 0.5 m/s larger than the inlet air flow. As time progresses, the cooling diffusion of the AHU shrinks the range of hot air and decreases the variation of air density in the room. About 300 s, a uniform temperature at 25 °C is distributed throughout the space; the direction of air flow is diagonal toward the air opening. The results show that the dead zone at the top-left side requires more time to approach the expected temperature. When the temperature gradient approaches zero as time progresses, the variation of air flow is still different. Although the applied fabric porous air duct can give a homogenous and small flow of inlet air, the air opening still dominates the direction and velocity of the air flow. The facility should be installed in this larger area of air flow to decrease the duration to attain a stable state of temperature.

In case two, the velocity distribution is similar to that of case 1 at time 300 s. The heat source blocks the air flow, which leads to a small velocity distribution and temperature gradient between the heat source and air openings. Figure 8 shows the temperature variation around the heat source in the direction from the heat source toward the air opening. The air flow caused by an arrangement of the inlet air duct and the air opening can guide the thermal gradient, which can be considered to avoid the coupling effect of waste heat.

Temperature stability related to space

We therefore adopted a fabric ductwork and diffuser and built a numerical model of simulation to analyze the effects of the arrangement of the inlet air duct and air opening. The fabric ductwork and diffuser are completely custom-made, from the engineering design to the manufactured product. At this time we chose a porous air duct to expect a great distribution of air flow in the space.

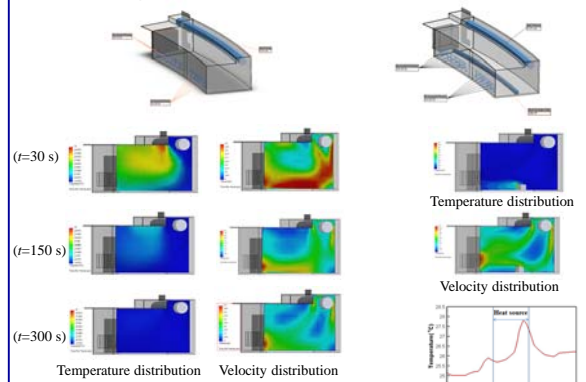


Figure 6: Temperature and velocity distributions as time progresses

Figure 8: Temperature gradient around the heat source